

NEW FINDING ON PRESSURE RESPONSE IN LONG, NARROW RESERVOIRS

Freddy-Humberto Escobar*¹, Oscar Muñoz¹, Jairo Sepúlveda¹ and Matilde Montealegre¹

¹Universidad Surcolombiana, Programa de Ingeniería de Petróleos, Grupo de Investigación en Pruebas de Pozos
e-mail: fescobar@usco.edu.co

(Received 3 March 2005; Accepted 1 November 2005)

During the process of reservoir characterization using well test analysis, before defining the reservoir model, it is convenient to properly identify flow regimes, which appear as characteristic patterns or “fingerprints” exhibited by the pressure derivative curve, because they provide the geometry of the streamlines of the tested formation. A set of reservoir properties can be estimated using only a portion of the pressure transient data of the flow regime. However, there are few cases with unidentified behaviors that deserve our attention.

The ten flow regime patterns commonly recognized in the pressure or pressure derivative curves of vertical or horizontal wells are: radial, spherical, hemispherical, linear, bilinear, elliptical, pseudosteady, steady, double porosity or permeability and doubled slope. A $\frac{1}{2}$ slope of the derivative trend is an indication of linear flow. If this shows up early, a hydraulic fractured well is dealt with, but if this shows up immediately after the radial flow regime an indication of a channel comes to our mind. A $-\frac{1}{2}$ -slope line at early times of the derivative plot indicates either spherical or hemispherical flow. However, if this line is observed once linear flow vanishes we are facing an unidentified flow regime.

We present the case of a channel reservoir with a well off-centered with respect to the extreme boundaries and close to a constant pressure boundary. At early times, the radial flow regime is observed and is followed by the linear flow regime. Once the open boundary is reached by the pressure disturbance, a $-\frac{1}{2}$ slope is observed on the pressure derivative plot and it lasts until the far extreme is felt. We simulated this behavior and plotted the isobaric lines and found out that a parabolic behavior shows up during this period of time. A typical behavior was found in Colombia in a reservoir of the Eastern Planes basin.

Keywords: image technique, linear flow regime, fluvial reservoirs, close boundaries, constante pressure boundaries, linear flow, radial flow, diffusivity equation.

* To whom correspondence may be addressed

Durante el proceso de caracterización de reservorio utilizando análisis de prueba de pozo, antes de definir el modelo de reservorio, es conveniente identificar correctamente los regímenes de flujo, los cuales aparecen como patrones característicos o “huellas digitales” que muestra la curva derivada de presión, porque proporcionan la geometría de las corriente de flujo (*streamlines*) de la formación probada. Se puede calcular un conjunto de propiedades de yacimiento utilizando apenas una porción de los datos transitorios de presión del régimen de flujo. Sin embargo, hay unos pocos casos con comportamientos no identificados que merecen nuestra atención.

Los diez patrones de régimen de flujo comúnmente reconocidos en la presión o curvas derivadas de presión de pozos verticales u horizontales son: radial, esférica, hemisférica, lineal, bilineal, elíptica, pseudoestable, estable, doble porosidad o doble permeabilidad y de doble pendiente. Una pendiente de $\frac{1}{2}$ de la tendencia de la derivada indica flujo lineal. Si ésto aparece a tiempos tempranos, se trata de un pozo hidráulicamente fracturado, pero si éste aparece inmediatamente después del régimen de flujo radial, pensamos en una indicación de canal. Una línea de pendiente $-\frac{1}{2}$ en los primeros tiempos del gráfico de la derivada es una indicación de flujo esférico o hemisférico. Sin embargo, si se observa esta línea una vez desaparece el flujo lineal, tenemos un régimen de flujo no identificado.

Presentamos el caso de un yacimiento alargado con un pozo descentrado con respecto a los límites extremos y cerca a una barrera de presión constante. En los primeros tiempos, se observa el régimen de flujo radial y lo sigue un régimen de flujo lineal. Una vez la perturbación de presión alcanza la frontera abierta, se observa una pendiente de $-\frac{1}{2}$ en el gráfico de la derivada de presión que continúa hasta que se siente el extremo más lejano. Simulamos este comportamiento y graficamos las líneas isobáricas y descubrimos que el comportamiento parabólico aparece durante este periodo de tiempo. Se encontró un comportamiento típico en Colombia en un yacimiento de la cuenca de los Llanos Orientales.

Palabras claves: método de las imágenes, régimen de flujo lineal, reservorios fluviales, fronteras cerradas, límites de presión constante, flujo lineal, flujo radial, ecuación de difusividad.

NOMENCLATURE

a_x	Distance from the real well to the left boundary
b_x	Distance from the real well to the right boundary
B	Oil volumetric factor
b_x	Distance from well to the closer lateral boundary, ft
b_y	Distance from well to the closer boundary in the y-direction, ft
c	Compressibility
h	Formation thickness
k	Permeability
P	Pressure
q	Flow rate
r_D	Dimensionless radius
r_{DR}	Dimensionless radius of real well
r_{DI}	Dimensionless radius at image well
$r_{L.n}$	Distance of n image wells on the left side
$r_{r.n}$	Distance of n image wells on the righth side
r_w	Well radius
s	Skin factor
t	Time
X_E	Reservoir length
X_D	Dimensionless well position
Y_E	Reservoir width
W_D	Dimensionless reservoir width

GREEK SYMBOLS

Δ	Change, drop
ΔP	Pressure drop
\emptyset	Porosity
μ	Viscosity
ρ	Fluid density

SUFFIXES

D	Dimensionless
D_L	Dimensionless linear
hs	Hemispherical
o	Oil
PB	Parabolic
t	Total
w	Well

INTRODUCTION

Modern well test interpretation techniques are based upon the appropriate identification of flow regimes observed on a log-log plot of pressure and pressure derivative (Abdelaziz and Tiab, 2004; Escobar *et al.*, 2003). The reservoir model is related to reservoir geology and petrophysics, and reservoir and well geometry, as well. Long, narrow reservoirs, for instance, have their own “fingerprint” on the pressure derivative plot. In these reservoirs, linear flow takes place once radial flow vanishes. Escobar *et al.* (2004), have presented a comprehensive well test interpretation technique using a pressure and pressure derivative plot for such systems without using type-curve matching (Tiab, 1994; Escobar *et al.*, 2004).

This paper introduces a new flow regime observed on channels reservoirs which we have named “Parabolic flow” because of the geometrical shape of its isobaric lines. (Figures 6 and 7). This flow regime takes place when a well (off-centered with respect to their far extreme boundaries) is near a constant pressure boundary. Once the pressure transient arrives there, parabolic flow (characterized by a -1/2-slope line on the pressure derivative curve) develops and lasts until the far boundary is felt. (Figures 1 and 2).

MATHEMATICAL FORMULATION

The source-line solution to the radial diffusivity equation in dimensionless form is given by Earlougher (1977):

$$P_D(r_D, t_D) = -\frac{1}{2} Ei \left[-\frac{r_D^2}{4t_D} \right] \tag{1}$$

Superposition principle is applied to obtain the pressure behavior of a well located inside a rectangular reservoir with lateral boundaries either constant pressure, no-flow or mixed. An infinite number of images (Ispas and Tiab, 1999; Rhagavan, 1993) are needed to reproduce the boundaries. For the constant pressure case the governing equation is given by Ispas and Tiab (1999):

$$P_D(x_{D1}, y_{D1}, t_D) = -\frac{q_1}{2q} Ei \left(-\frac{r_{D1}^2}{4t_D} \right) - \frac{q_2}{2q} Ei \left(-\frac{r_{D2}^2}{4t_D} \right) \tag{2}$$

Assuming $q = q_1 = -q_2$, Equation 2 becomes:

$$P_D(x_{D1}, y_{D1}, t_D) = -\frac{1}{2} \left[Ei \left(-\frac{r_{D1}^2}{4t_D} \right) - Ei \left(-\frac{r_{D2}^2}{4t_D} \right) \right] \tag{3}$$

Let $r_{L,n}$ and $r_{r,n}$ be the distance between the real well and a particular image well on both left and right sides of the reservoir:

$$r_{L,n} = r_{L,(n+1)} + [1 - (-1)^n] a_x + [1 - (-1)^n] b_x \tag{4}$$

$$r_{r,n} = r_{r,(n+1)} + [1 - (-1)^n] b_x + [1 - (-1)^n] a_x \tag{5}$$

The dimensionless distances from the image well are:

$$r_{DIL,n} = \frac{r_{L,n}}{X_E} \tag{6}$$

$$r_{Dlr,n} = \frac{r_{r,n}}{X_E}$$

Let $G_{L,n}$ as the symbol to define the n well images on the left side and $G_{r,n}$ the symbol to define the n well images on the right side. Their values are +1 for a production well and -1 for an injection well.3

Case 1. Two constant pressure boundaries

According to the image technique, the type of image changes when flow is generated. Then, not all images are the same type as the real well. In other words, if the real well is on production the image will be an injector and so on. The terms have the same variation at both sides, thus:

$$G_{L,n} = G_{r,n} = (-1)^n$$

The pressure and pressure derivative are given by:

$$P_D(r_D, t_{DA}) = -\frac{1}{2} \left[Ei \left(-\frac{r_{DR}^2}{4t_{DA}} \right) + \sum_{n=1}^{\infty} G_{L,n} \left[Ei \left(-\frac{r_{DIL,n}^2}{4t_{DA}} \right) + Ei \left(-\frac{r_{Dlr,n}^2}{4t_{DA}} \right) \right] \right] \tag{8}$$

$$P'_D(r_D, t_{DA}) = -\frac{1}{2t_{DA}} \left[\exp \left(-\frac{r_{DR}^2}{4t_{DA}} \right) + \sum_{n=1}^{\infty} G_{L,n} \left[\exp \left(-\frac{r_{DIL,n}^2}{4t_{DA}} \right) + \exp \left(-\frac{r_{Dlr,n}^2}{4t_{DA}} \right) \right] \right] \tag{9}$$

Case 2. Mixed boundaries (a constant pressure and no-flow boundary)

Let $G_{F,n}$ the symbol to define the n well images on the flow and $G_{NF,n}$ the symbol to define the n well images on the no flow boundary. We have:

$$G_{F,n} \neq G_{NF,n} \tag{10}$$

$$G_{F,n} = (-1)^n G_{F,(n-1)} \tag{11}$$

$$G_{NF,n} = (-1)^{(n-1)} G_{NF,(n-1)} \tag{12}$$

The pressure and pressure derivative expressions are given by:

$$P_D(r_D, t_{DA}) = -\frac{1}{2} \left[E_i \left(-\frac{r^2}{4t_{DA}} \right) + \sum_{n=1}^{\infty} \left[G_{L,n} E_i \left(-\frac{r_{DL,n}^2}{4t_{DA}} \right) + G_{r,n} E_i \left(-\frac{r_{Dr,n}^2}{4t_{DA}} \right) \right] \right] \tag{13}$$

$$P'_D(r_D, t_{DA}) = -\frac{1}{2t_{DA}} \left[\exp \left(-\frac{r^2}{4t_{DA}} \right) + \sum_{n=1}^{\infty} \left[G_{L,n} \exp \left(-\frac{r_{DL,n}^2}{4t_{DA}} \right) + G_{r,n} \exp \left(-\frac{r_{Dr,n}^2}{4t_{DA}} \right) \right] \right] \tag{14}$$

Equations 7 through 14 were used to generate a set of type curves considering several reservoir situations and well positions. Among these, Figures 1 and 2 are reported.

WELL PRESSURE BEHAVIOR AND FLOW REGIMES

The pressure derivative plot is the best tool to identify the different flow regimes taking place in any reservoir. Figure 1 contains a set of type curves for channelized reservoirs with both lateral boundaries at constant pressure and Figure 2 presents type curves for the same reservoirs, with the near boundary open to flow and the far one of no-flow. In both cases, the pressure behavior is the same until the disturbance reaches the far extreme or boundary. In Figure 1, steady state develops immediately after reaching the far boundary. In Figure 2, the pressure derivative slightly rises as a consequence of feeling the no-flow boundary but it goes down as the constant pressure boundary dominates the test.

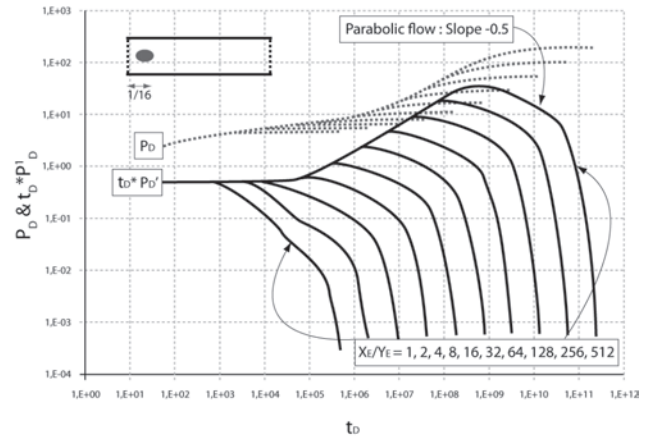


Figure 1. Pressure and pressure derivative behavior of a long reservoir with both lateral sides at constant pressure

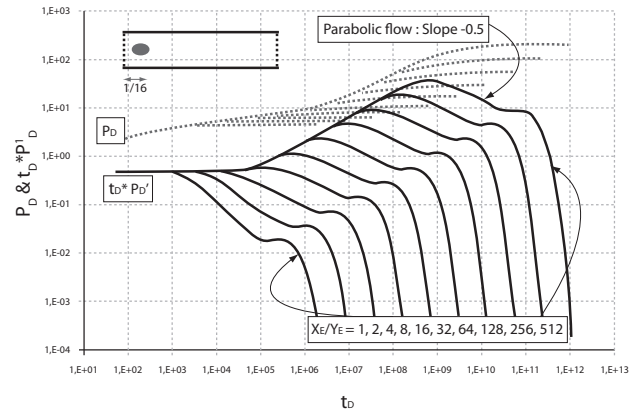


Figure 2. Pressure and pressure derivative behavior of a long reservoir with the near boundary open and the far boundary closed

A simulated test in a rectangular reservoir was conducted with a commercial numerical simulator using the information given in Table 2. It is valid to say that simulations were not achieved by using the method of the images. Because of round-off and truncation errors and the relative small number of PEBI cells used, the isobaric lines are not well smoothed as seen in Figures 4 through 7. Also, we must take into account that the contouring software was unable of generating the isobaric plot so the orthogonality condition between the isobars and the close boundary could be satisfied. This situation could overcome by performing a local grid refinement along the boundaries, so a great number of cells, then pressure values, can be better represented and plotted. However, commercial numerical simulators normally refine the

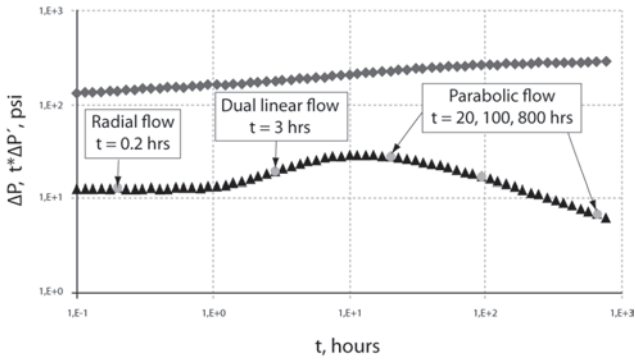


Figure 3. Simulated well pressure test

PEBI grid around the well. However, for practical purposes, our attempt was to show the overall shape of the profile. Isobaric lines were plotted at certain given times during the test where specific flow regimes were developed. The following flow regimes are observed:

Radial flow

It is observed at early time and characterized for a zero-slope line intersecting the dimensionless pressure



Figure 4. Isobaric lines during radial flow, $t = 0,2$ h.



Figure 5. Isobaric lines during dual linear flow, $t = 3$ h.

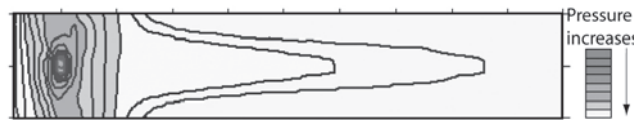


Figure 6. Isobaric lines during parabolic flow, $t = 20$ h.

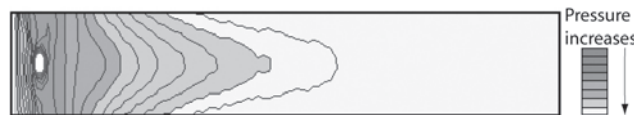


Figure 7. Isobaric lines during parabolic flow, $t = 100$ h.

Table 1. Reservoir and fluid properties for field case example

Property	Value
Approximate channel-well configuration	
Formation thickness, h , ft	14
Reservoir permeability, k , md	441
Distance from well to closer boundary, b_x , ft	285
Channel width, Y_E , ft	360
Channel length, X_E , ft	637
Viscosity, μ , cp	3,5
Oil volume factor, B , bbl/STB	1,07
Well radius, r_w , ft	0,51
Oil flow rate, q , BPD	1400
Porosity, ϕ , fracción	0,24
Total compressibility, c_t , psi^{-1}	9×10^{-6}

derivative axis at a value of 0,5. Figure 4 shows the isobaric lines for this regime built at a time, $t = 0,2$ h, which really corresponds to a radial flow regime as seen on the simulated test of Figure 3. Streamlines (arrows) are orthogonal to the isobaric lines (dotted lines) and converge together toward the well as depicted in Figure 8.

Dual linear flow

This flow regime, also called linear flow in two directions, is recognized by a $1/2$ -slope line on the pressure derivative curve. Figure 8 also sketches this flow regime which was first introduced by Wong *et al.* (1986) and

Table 2. Input data for simulation

Property	Value	Property	Value
Initial reservoir pressure, P_i , psia	4000	Rock compressibility, c_r , psi ⁻¹	1×10^{-6}
Formation thickness, h , ft	100	Permeability, k , md	100
Viscosity, μ , cp	2	Oil density, ρ , lb/ft ³	52
Oil volume factor, B , bbl/STB	1,05	Wellbore storage, C , bbl/psi	0
Well radius, r_w , ft	0,35	Skin factor, s	0
Flow rate, q , BPD	850	Reservoir width, Y_E , ft	500
Porosity, ϕ , fracción	0,20	Reservoir length, X_E , ft	9500
Total compressibility, c_t , psi ⁻¹	3×10^{-6}		

Tiab (1993). For us who use the TDS technique 1-5, it is truly important to properly identify this flow regime for an accurate reservoir characterization as outlined in Escobar *et al.* (2004). Isobaric lines flow linearly

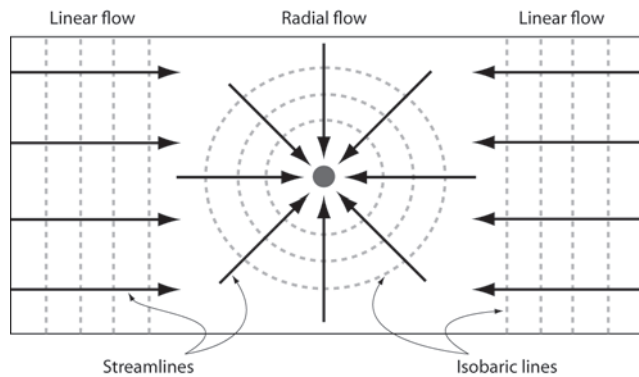


Figure 8. Schematic representation of linear and radial flow regimes

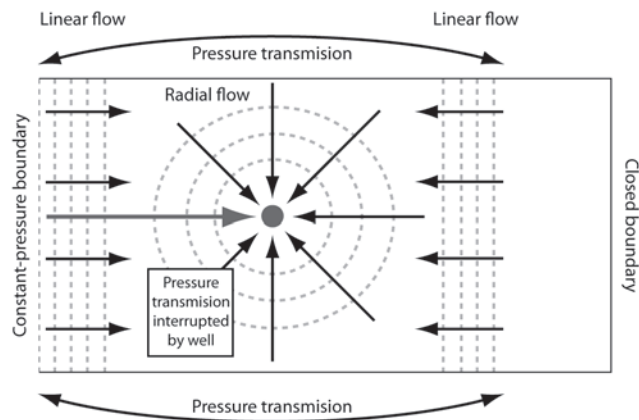


Figure 9. Ending of dual linear flow regime and beginning of parabolic profile

at opposite sides of the well from the reservoir sides. (Figure 5). This plot was constructed at a time, $t = 3$ h of Figure 3. This is very typical of long reservoirs and masks the single linear flow when the well is centered with respect of the extreme boundaries.

Parabolic flow

This flow regime, characterized by a $-1/2$ -slope line on the derivative plot, takes place when the well is near a constant pressure boundary and the pressure disturbance reaches it. A simultaneous action of the expected single linear flow and the steady-state flow is observed as depicted in Figures 6, and 7 which isobaric lines were built at times, $t = 20$, and 100 h, respectively. We believe that the constant pressure boundary dominates the transient behavior pressure but its effect is interrupted by the presence of the well as sketched in Figure 9. Then linear parallel isobaric lines have to be deformed as shown in Figure 10, therefore, the higher pressure drop is seen on the right side of the well at the center of the reservoir. At these points, pressure from the left side

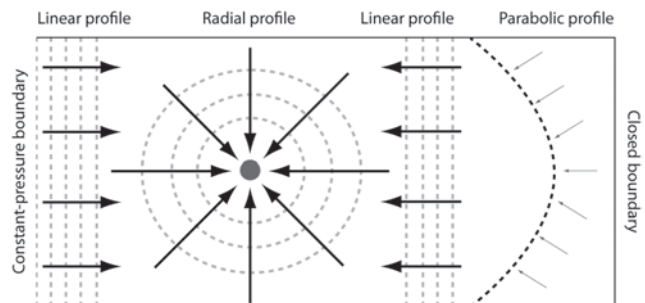


Figure 10. Hypothetical representation of the parabolic

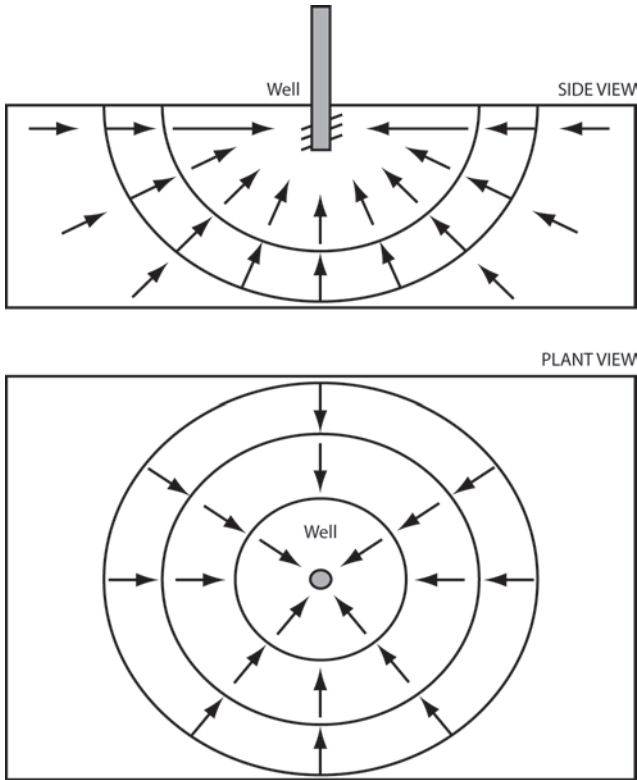


Figure 11. Sketch of hemispherical flow

of the well is hard to be transmitted to the right one. A field case pressure test conducted in a Colombian reservoir displays this flow regime as shown in Figure 12. Basic information for this reservoir is given in Table 1. This test was simulated with a commercial well testing package and successfully represented by the reservoir configuration presented in the first row of Table 1. The results were successfully compared to those obtained from the application of the TDS technique as presented in Escobar *et al.* (2004).

Pseudosteady state flow

This takes place when all the reservoir boundaries are close and a one-slope line is observed on the derivative curve. If the test is very long pressure and pressure derivative lines become a single one. This is not shown in any of the type curves provided in this study. However, it tries to develop, (Figure 2) once the far close boundary is reached by the disturbance but the steady-state from the left side dominates the test and pressure derivative goes down. According to our observations, parabolic profile does not develop if pseudosteady state exists in channelized reservoirs.

Steady-state flow

Once the transient reaches the right constant pressure boundary, (Figure 1), this state dominates the test. Pressure begins to remain constant at certain points of the reservoir, and therefore, no change in pressure takes place. Because of this, pressure derivative abruptly decreases (Figures 1 and 2).

WELL PRESSURE MODEL

The dimensionless time, pressure and pressure derivative are given by Earlougher (1977):

$$t_D = \frac{0.0002637kt}{\phi\mu c_r r_w^2} \tag{15}$$

$$P_D = \frac{kh}{141.2q\mu B} \Delta P \tag{16}$$

$$t_D * P_D' = \frac{kh}{141.2q\mu B} (t * \Delta P') \tag{17}$$

According to Joseph (1984), the pressure and pressure derivative behavior for hemispherical flow are given by:

$$P_D = 1 - \frac{1}{\sqrt{\pi t_D}} + s_{hs} \tag{18.a}$$

$$(t_D * P_D') = \frac{1}{2\sqrt{\pi}} t_D^{-1/2} \tag{18.b}$$

Streamlines and isobaric lines for this case are sketched in Figure 11. Define the dimensionless time, width and well position for a channel-type reservoir, respectively, as:

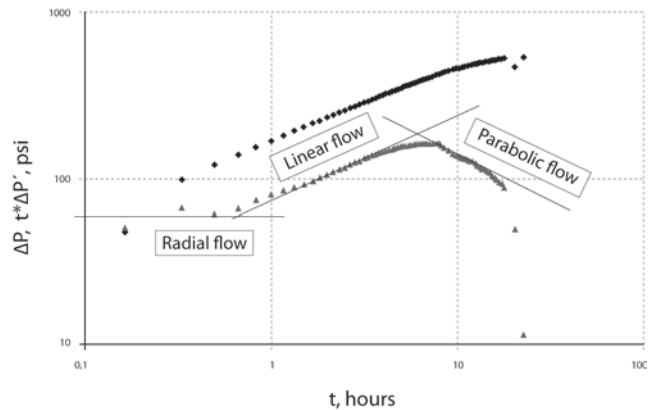


Figure 12. Log-log plot of pressure and pressure derivative of a real pressure test of a channelized reservoir located in Colombia

$$t_{D_L} = \frac{t_D}{W_D^2} \quad (19.a)$$

$$W_D = \frac{Y_E}{r_w} \quad (19.b)$$

$$X_D = \frac{2b_x}{X_E} \quad (19.c)$$

$$Y_D = \frac{2b_y}{Y_E} \quad (19.d)$$

According to Escobar *et al.* (2004), the governing pressure and pressure derivative equations for the new flow regime matter of this study are:

$$P_D = -(W_D)(X_D)^2 \left(\frac{X_E}{Y_E} \right)^2 t_D^{-0.5} + s_{PB} \quad (20.a)$$

$$t_D * P'_D = \frac{W_D}{2} (X_D)^2 \left(\frac{X_E}{Y_E} \right)^2 t_D^{-0.5} \quad (20.b)$$

As shown in Tiab and Crichlow (1979), and Wong *et al.* (1986), the pressure behavior is a function of time to the power 0,36 for elliptical flow. A pressure profile for a horizontal well during the elliptical flow regime is shown in Figure 1 of Wong *et al.* (1986). Although, the time dependence of pressure in *Equations 18.a* and *20.a* are the same, these two equations are not alike. Therefore, the behavior of the pressure as dealt in this study is neither hemispherical nor elliptical and the isobaric lines show that the closest geometrical shape corresponds to a parabol.

CONCLUSIONS

- A new flow regime, called here “parabolic flow”, has been identified and observed in long, narrow reservoirs when the well is near an open boundary. This has a -1/2-slope line observed on the pressure derivative curve and it is the result of the action from the constant pressure at the near side of the reservoir on the portion of the reservoir opposite to the near boundary where linear flow was expected to be developed.
- The pressure behavior of a -1/2-slope line found on the pressure derivative plot shows up after the dual-linear regime vanishes and cannot be seen if late pseudosteady-state regime exists.

ACKNOWLEDGMENTS

The authors gratefully acknowledge the financial support of the Instituto Colombiano del Petróleo (ICP), under the mutual agreement Number 008 signed between this institution and Universidad Surcolombiana.

REFERENCES

- Abdelaziz, B. and Tiab, D., “Pressure Behaviour of a Well Between Two Intersecting Leaky Faults”. *Nigeria Annual International Conference and Exhibition*, Aug. 2-4. Abuja, Nigeria, SPE 88873.
- Earlougher, R.C., Jr., 1977. “Advances in Well Test Analysis”, *Monograph Series 5*, SPE, Dallas, TX., USA.
- Escobar, F.H., Muñoz, O.F. and Sepúlveda J.A., 2004. “Horizontal Permeability Determination from the Elliptical Flow Regime for Horizontal Wells”. *CT&F – Ciencia, Tecnología y Futuro*, 2 (5): 83-95.
- Escobar, F.H., Saavedra, N.F., Hernández, C.M., Hernández, Y.A., Pilataxi, J.F., and Pinto, D.A., 2004. “Pressure and Pressure Derivative Analysis for Linear Homogeneous Reservoirs without Using Type-Curve Matching”. *28th Annual SPE International Technical Conference and Exhibition*, Abuja, Nigeria, Aug. 2-4. SPE 88874.
- Escobar, F.H., Tiab, D. and Jorkhio, S.A., 2003. “Characterization of Leaky Boundaries from Transient Pressure Analysis”. *Production and Operations Symposium*, Oklahoma City, Oklahoma, U.S.A., March 23-25. SPE 80908.
- Ispas, V., and Tiab, D., 1999. “New Method of Analyzing the Pressure behavior of a Well Near Multiple Boundary System”. *Latin American and Caribbean Petroleum Engineering Conference*, Caracas, Venezuela, April 21-23. SPE 53933.
- Joseph, J.A., 1984. “Unsteady-State Cylindrical, Spherical and Linear flow in Porous Media” *Ph.D. Dissertation*, University of Missouri-Rolla.
- Rhagavan, R., 1993. “*Well Test Analysis*”. Prentice Hall. New Jersey.
- Tiab, D., 1993. “Analysis of Pressure and Pressure Derivative without Type-Curve Matching: 1- Skin Factor and Wellbore Storage”. *Production Operations Symposium*,

Oklahoma City, OK., March 21-23. SPE 25423, 203-216.
Also, *J. Petroleum Scien. and Engineer.*, 171-181.

Tiab, D., 1994. "Analysis of Pressure Derivative without Type-Curve Matching: Vertically Fractured Wells in Closed Systems". *J. Petroleum Scien. and Engineer.*, 323-333.

Tiab, D., Azzougen, A., Escobar, F. H., and Berumen, S., 1999. "Analysis of Pressure Derivative Data of a Finite-Conductivity Fractures by the 'Direct Synthesis Technique'." Mid-Continent Operations Symposium Oklahoma City, OK., March 28-31. SPE 52201: *Latin American and Caribbean Petroleum Engineering Conference*, Caracas, Venezuela, April 21-23.

Tiab, D. and Crichlow, H., 1979. "Pressure Analysis of Multiple-Sealing-Fault Systems and Bounded Reservoirs by Type-Curve Matching". *J. Petroleum Scien. and Engineer.*, 378-392.

Wong, D.W., Mothersele, C.D., Harrington, A.G. and Cinco-Ley, H., 1986. "Pressure Transient Analysis in Finite Linear Reservoirs Using Derivative and Conventional Techniques: Field Examples" *61st Annual technical Conference and Exhibition of the Soc. of Petroleum Engineers.*, New Orleans, LA., SPE 15421.